Korean J. Chem. Eng., 33(3), 782-794 (2016)
DOI: 10.1007/s11814-015-0214-8

pISSN: 0256-1115
eISSN: 1975-7220

A numerical study on the performance evaluation of ventilation systems for indoor radon reduction

Ji Eun Lee, Hoon Chae Park, Hang Seok Choi†, Seung Yeon Cho, Tae Young Jeong, and Sung Cheoul Roh

Department of Environmental Engineering, Yonsei University, Wonju 220-710, Korea
(*Received 10 June 2015 • accepted 11 October 2015*)

Abstract−Numerical simulations were conducted using computational fluid dynamics to evaluate the effect of ventilation conditions on radon (^{222}Rn) reduction performance in a residential building. The results indicate that at the same ventilation rate, a mechanical ventilation system is more effective in reducing indoor radon than a natural ventilation system. For the same ventilation type, the indoor radon concentration decreases as the ventilation rate increases. When the air change per hour (ACH) was 1, the indoor radon concentration was maintained at less than 100 Bq/m^3. However, when the ACH was lowered to 0.01, the average indoor radon concentration in several rooms exceeded 148 Bq/m^3. The angle of the inflow air was found to affect the indoor air stream and consequently the distribution of the radon concentration. Even when the ACH was 1, the radon concentrations of some areas were higher than 100 Bq/m^3 for inflow air angles of 5° and 175°.

Keywords: Computational Fluid Dynamics, Exhalation, Indoor Air, Radon, Ventilation

INTRODUCTION

Radon (^{222}Rn) is a naturally occurring radioactive gas generated by the disintegration of the uranium that exists in soil and rocks. It has a half-life of 3.8 days, and as radon decays, new radioactive elements (^{218}Po, ^{214}Pb, ^{214}Bi, and ^{214}Po) called radon progenies are produced. They are chemically active and radioactive. When radon decays, it also emits an alpha particle of 5.5-MeV energy. It has been proven that a significant relationship exists between long-term exposure to radon, along with its short-lived progenies, and lung cancer. Therefore, it is classified as a carcinogenic substance [1-3]. Indoor radon originates in soil and is released at building sites and from building materials [4]. Indoor radon concentrations must be maintained under regulatory limits because of radon's potential to cause harm. Therefore, it is necessary to identify effective ventilation systems and optimal ventilation conditions to improve indoor air quality by reducing indoor radon concentrations.

Experiments or numerical simulation methods can be used to predict the behavior and distribution of indoor air pollutants [5,6]. Computational fluid dynamics (CFD) has been widely used for this purpose because it offers several advantages. It is especially beneficial in the study of pollutants whose generation is difficult to control or that are very noxious even at low concentrations. Various studies have used numerical methods to study indoor air pollutants and ventilation systems. Many researchers have also utilized numerical methods to study indoor radon. Fang and Persily [7] predicted the characteristics of air flow and radon concentrations in large buildings, such as apartment buildings, office buildings, and schools, using computer simulations. Zhuo et al. [8] simulated the concentration and distribution of radon and thoron in a model room. Wang et al. [9] used CFD to develop a model for entry of radon into a house cellar. The effects of the air change rate, temperature, and humidity on the indoor radon concentrations in a detached house were studied by Akbari et al. [10].

However, in spite of its importance, the evaluation of ventilation regulation for radon has not been fully studied. Furthermore, studies on the prediction of indoor radon distribution and the radon reduction performance of ventilation systems for various ventilation conditions have rarely been carried out using CFD. Therefore, in the present study, CFD simulations were carried out to predict the distribution of indoor radon concentrations and to estimate the effects of a ventilation system on indoor radon reduction. The American Society of Heating, Refrigerating and Air-conditioning Engineers, Inc. (ASHRAE) and World Health Organization (WHO) standards were used to evaluate the ventilation performance of a typical Korean house.

CALCULATION METHODS

1. Governing Equations

Reynolds-averaged Navier-Stokes (RANS) equations were applied in this study. An incompressible steady-state turbulent flow was assumed in the calculation of the air flow field and the evolution of the indoor radon concentration. The time-averaged continuity equation, momentum equation, and chemical species transport equation were solved.

The governing equations are as follows:

- Continuity equation:

$$\frac{\partial U_i}{\partial x_i} = 0 \tag{1}$$

where U_i is the mean velocity vector for the i direction;

†To whom correspondence should be addressed.
E-mail: hs.choi@yonsei.ac.kr

- Momentum equation:

$$\frac{\partial}{\partial x_j}(\rho U_i U_j) = -\frac{\partial P}{\partial x_i} + \frac{\partial}{\partial x_j}\left(\mu\frac{\partial U_i}{\partial x_j} - \rho\overline{u_i' u_j'}\right) \quad (2)$$

where ρ is the density, P is the mean pressure, μ is the dynamic viscosity, and $-\rho\overline{u_i' u_j'}$ in Eq. (2) is the Reynolds stress tensor, which can be calculated by turbulence modeling;

- Species equation:

$$\frac{\partial}{\partial x_j}(\rho U_j Y_i) = -\left(\frac{\partial}{\partial x_j} J_i\right) + S_i \quad (3)$$

and

$$J_i = -\rho D_{i,m} \nabla Y_i \quad (4)$$

where Y_i and J_i are the mass fraction and diffusion flux of species i, respectively, S is the source term, and $D_{i,m}$ is the diffusion coefficient of chemical species i in the gas mixture.

As discussed above, to solve Eq. (2), the Reynolds stress tensor should be modeled. In the present study, the Reynolds stress tensor was modeled as follows:

$$-\rho\overline{u_i' u_j'} = \mu_t\left(\frac{\partial U_i}{\partial x_j} + \frac{\partial U_j}{\partial x_i}\right) - \frac{2}{3}\rho k\delta_{ij} \quad (5)$$

where the realizable k-ε model was used to calculate the turbulent kinetic energy and its dissipation rate in Eq. (5). The transport equations for the turbulent kinetic energy and its dissipation rate are as follows:

- Turbulent kinetic energy, k, equation:

$$\frac{\partial}{\partial x_j}(\rho\kappa U_j) = \frac{\partial}{\partial x_j}\left[\left(\mu + \frac{\mu_t}{\sigma_\kappa}\right)\frac{\partial \kappa}{\partial x_j}\right] + G_\kappa - \rho\varepsilon \quad (6)$$

$$G_\kappa = \mu_t\left(\sqrt{2S_{ij}S_{ji}}\right)^2 \quad (7)$$

$$\mu_t = \lambda(\mu_t)_{\kappa-\varepsilon} + (1\varepsilon\lambda)\mu\left(\frac{\mu_t}{\mu}\right)_{2\ layer} \quad (8)$$

$$\lambda = \frac{1}{2}\left[1 + \tanh\left(\frac{Re_y - 60}{A}\right)\right] \quad (9)$$

and

$$A = \frac{|\Delta Re_y|}{\tanh 0.98} \quad (10)$$

where G_k in Eq. (6) is the turbulent kinetic energy generated by the mean velocity gradient, defined in Eq. (7); S_{ij} is the strain rate tensor; and Re_y is the wall-distance Reynolds number. In this study, the realizable k-ε model was applied with the two-layer wall treatment approach. Therefore, the turbulent viscosity, which is expressed as μ_t, was blended with the two-layer value and defined in Eqs. (8), (9), and (10) as follows:

- Turbulent dissipation rate, ε, equation:

$$\frac{\partial}{\partial x_j}(\rho\varepsilon U_j) = \frac{\partial}{\partial x_j}\left[\left(\mu + \frac{\mu_t}{\sigma_\varepsilon}\right)\frac{\partial \varepsilon}{\partial x_j}\right] + C_{\varepsilon 1}\sqrt{2S_{ij}S_{ji}}\varepsilon - C_{\varepsilon 2}\rho\frac{\varepsilon^2}{\kappa} \quad (11)$$

$$C_{\varepsilon 1} = \max\left(0.43, \frac{\sqrt{2S_{ij}S_{ji}}\kappa/\varepsilon}{5 + \sqrt{2S_{ij}S_{ji}}\kappa/\varepsilon}\right) \quad (12)$$

$$C_{\varepsilon 2} = 1.9 \quad (13)$$

$$\sigma_\kappa = 1.0 \quad (14)$$

and

$$\sigma_\varepsilon = 1.2 \quad (15)$$

In Eq. (11), the constants are given in Eqs. (12)-(15).

2. Calculation Conditions

It is difficult to generalize houses with a computational model because their shapes, sizes, and inner structures are very diverse. Therefore, the house in the present study was modeled based on statistical data for houses in South Korea. Fig. 1(a) shows the three-dimensional computer-aided design (CAD) model of the house that was used for the calculations. In addition, mechanical ventilation systems were loaded into the model. The number of household members who lived in the house was assumed to be the average number of household members in South Korea (2.7 people), which was rounded up to three people [11]. The house type selected was an apartment, which is the most common type in South Korea.

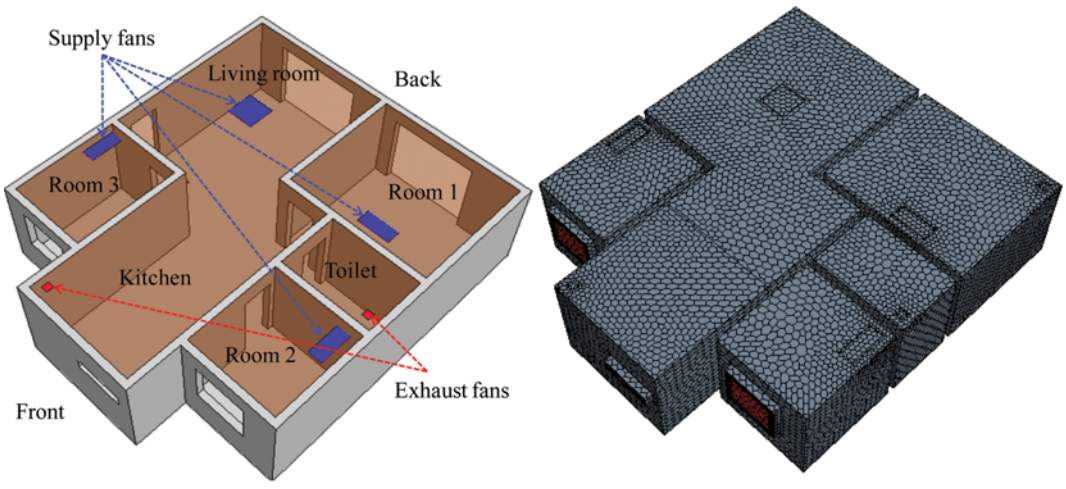

(a) House plan (b) Grid structure

Fig. 1. Computational domain.

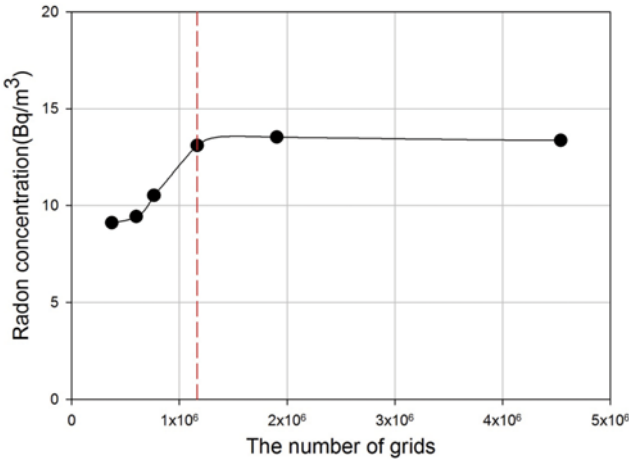

Fig. 2. Results of the grid dependency test.

Table 1. Properties of the chemical species at the standard condition

Property	Air	Radon
Molecular weight (kg/kmol)	28.9664	222
Density (kg/m^3)	1.18415	9.37
Dynamic viscosity (kg/m-s)	1.85508×10^{-5}	1.8×10^{-5}

Table 2. Radon exhalation rate according to the building and interior materials

Material	Radon exhalation rate (Bq/m^2-h)	Area
Concrete	2.89	Floor and walls
Gypsum board	2.53	Ceiling
Tile	0.34	Toilet floor and walls

The number of apartments in South Korea is 8,308,021, out of a total of 17,733,831 households, according to the governmental statistics report for the 2012 national survey of residence status in South Korea [12]. The size of the house was determined to be 78.10 m^2, which is also the national average size, based on the statistics. Taking into consideration the size of the house and the number of household members, the house was modeled to consist of three bedrooms, a toilet, a kitchen, and a living room. However, because there were no standard or specific supporting data for an inner structure and a house plan, these were chosen subjectively by considering sample plans for a 79.33 m^2 apartment building from several construction firms. For the mechanical ventilation, exhaust fans were located in the kitchen and the toilet. In Fig. 1(a), the exhaust fans are marked in red. In addition, supply fans were located in the living room and each of the bedrooms, and they are marked in blue in the figure. Fig. 1(b) shows the computational grid structures of the calculation domain. Approximately 120,000 polyhedral meshes were used. It is very important to find the optimal number of grids that does not adversely affect the accuracy of the calculation. Therefore, a grid dependency test was performed before the main calculations were performed to minimize the error associated with the number of grids. Fig. 2 indicates that the radon concentration remains constant when the number of grids is more than 120,000. Increasing the number of grids increases the calculation time and cost. Therefore, in the current study, computational analysis was performed using the minimum number of grids determined from the grid dependency test.

For the standard conditions (101.3 kPa, 273 K), the chemical and physical properties of air and radon are given in Table 1. In this study, the turbulent convective air flow was the most dominant factor in the passive scalar evolution. Therefore, the effects of the other gas species in the air on the diffusion of the indoor radon were assumed to be negligible. The radon exhalation rates of the building and interior materials, with areas where the materials were applied, are presented in Table 2. The radon exhalation rate of each construction material was measured using continuous radon monitoring equipment (RTM 1688-2, Silicon Surface-Barrier Detector) in an airtight acrylic container for ten hours [13]. The materials are the types primarily used for houses in South Korea. The compositions of the materials used for the house were selected based on the results of previous studies [14,15]. Therefore, the house in this study was assumed to consist of those materials, and their radon exhalation rates were applied.

The ASHRAE Standard 62.1 suggests ventilation standards for buildings to meet indoor air quality regulations. This standard requires consideration of the volume or area of a house and the number of occupants. In addition, an exhaust rate should be included for special-purpose zones in a house, such as the kitchen and toilet [16]. Taking into consideration the criteria noted above, three different ventilation types were selected and evaluated in the present study. The types of ventilation and the inlet and outlet positions are presented in Table 3. Both natural supply and exhaust ventilation occurred in cases 1 and 2; the difference between cases 1 and 2 was the inlet for air flow. In contrast with mechanical ventilation, the direction of a natural air supply cannot be controlled artificially; it follows the direction of the wind, which is inconsistent. In case 1, the windows located on the front side of the house (room 2, the kitchen, and room 3) were air inlets. On the other hand, the windows in case 2 that were located on the back side of the house (room 1 and the living room) were inlets for air. In case 3, only mechanical exhaust and supply ventilation occurred. The

Table 3. Calculation conditions

Case	Ventilation type	Inlet position	Outlet position
1	Natural	- Windows of Room2, Room3, and Kitchen	- Windows of Room1 and Living room
2	Natural	- Windows of Room1 and Living room	- Windows of Room2, Room3, and Kitchen
3	Mechanical	- Supply fans located at the ceilings of Room1, Room2, Room3, and Living room	- Exhaust fans located at the ceiling of Kitchen and Toilet

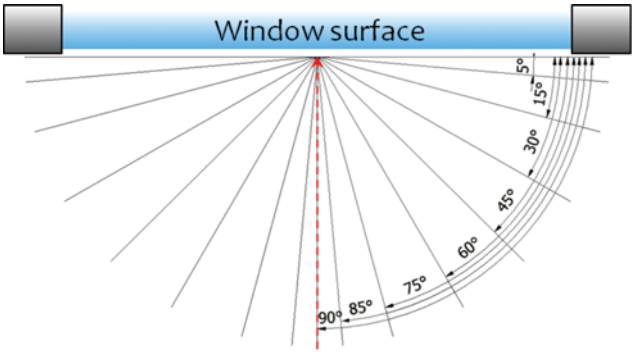

Fig. 3. Angle of inflow air through windows.

flow direction of natural wind is not fixed and cannot be controlled. Therefore, the angle of inflow air through windows is not always perpendicular to the window. When natural ventilation occurs, the effects of the angle of air flow on indoor radon reduction need to be considered. Therefore, various angles of inflow air through the windows were applied as boundary conditions for different air change rates. Fig. 3 shows the inflow angles between the window front surface and the outdoor air that flows into the house. The inflow angle is defined as increasing in the clockwise direction from 0° (parallel to the window) to 90° (perpendicular to the window).

The distribution of the indoor radon concentration and the indoor radon reduction performance were scrutinized for a range of ventilation rates. Ventilation rates are commonly expressed as air change per hour (ACH). The ventilation rate that meets the ASHRAE Standard 62.1 is approximately 1 ACH [16]. The regulation of indoor ventilation in South Korea is legislated by Article 11 (the ventilation standard for an apartment and a public facility) in Ordinance 23 of the Ministry of Land, Infrastructure, and Transport (equipment standards of a building). According to this law, an apartment building that has more than 100 units is required to have a natural or mechanical ventilation system installed to ventilate the indoor air at least 0.5 times per hour [17]. The ventilation efficiency and indoor radon concentration as a function of the ACH were compared and scrutinized. Table 4 shows the conditions of the air change rate. Three ventilation systems were considered for each air change rate.

The yearly average and variation of the wind velocity in South Korea are presented in Fig. 4. The minimum wind velocity is approximately 1.4 m/s throughout South Korea. Therefore, in reality, the maximum inlet air velocity, 0.014 m/s, which was applied in this study under the natural ventilation condition could be ensured [18]. The maximum inlet velocity of 0.014 m/s is the area-averaged velocity at the front windows of the house when the ACH is 1. ACH is defined as the portion of the total volume of air inside the house that is replaced by a volume of outside air per hour. Normally, 1 ACH is adequate to meet ventilation requirements. In this study, the air velocity was calculated on the basis of ACH value. The volume of the house was assumed to be 277.37 m^3, and the areas of the front and rear windows were taken to be 4.02 m^2

Table 4. Calculation condition for air change rate

ACH	Inflow air velocity on window (m/s)		Exhaust and supply air velocity (m/s)		Notes
			Case3		
	Case1	Case2	Supply	Exhaust	
1	1.46e-02	5.18e-03	- Room1: 3.19e-02 - Room2: 1.51e-02 - Room3: 1.50e-02 - Living room: 4.83e-02	- Kitchen: 7.34e-01 - Toilet: 7.34e-01	Ventilation standard of ASHRAE 62.1
0.5	7.30e-03	2.59e-03	- Room1: 1.59e-02 - Room2: 7.57e-03 - Room3: 7.49e-03 - Living room: 2.41e-02	- Kitchen: 3.67e-01 - Toilet: 3.67e-01	1/2 of ventilation standard of ASHRAE 62.1 and regulation of ventilation in South Korea
0.25	3.65e-03	1.30e-03	- Room1: 7.97e-03 - Room2: 3.78e-03 - Room3: 3.75e-03 - Living room: 1.21e-02	- Kitchen: 1.83e-02 - Toilet: 1.83e-02	1/4 of ventilation standard of ASHRAE 62.1 and 1/2 of regulation of ventilation in South Korea
0.1	1.46e-03	5.18e-04	- Room1: 3.19e-03 - Room2: 1.51e-03 - Room3: 1.50e-03 - Living room: 4.83e-03	- Kitchen: 7.34e-02 - Toilet: 7.34e-02	1/10 of ventilation standard of ASHRAE 62.1 and 1/5 of regulation of ventilation in South Korea
0.01	1.46e-04	5.18e-05	- Room1: 3.19e-04 - Room2: 1.51e-04 - Room3: 1.50e-04 - Living room: 4.83e-04	- Kitchen: 7.34e-03 - Toilet: 7.34e-03	1/100 of ventilation standard of ASHRAE 62.1 and 1/50 of regulation of ventilation in South Korea

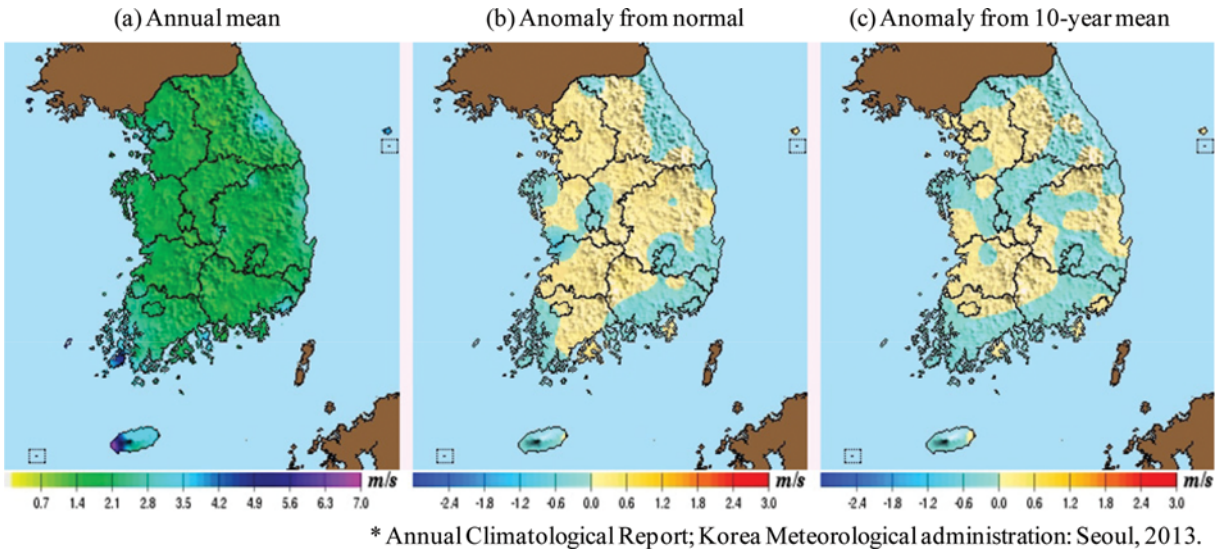

Fig. 4. Mean wind speed distribution in the southern portion of the Korean peninsula.

Table 5. Boundary conditions

Boundary	Condition
Inlet	- Dirichlet (constant velocity)
Outlet	- Dirichlet (constant pressure)
Wall	- No-slip - Dirichlet (constant radon exhalation rate)

and 11.33 m^2, respectively. For the above dimensions and an ACH of 1, the air velocities at the front and rear windows were calculated to be 0.014 and 0.005 m/s, respectively.

Table 5 shows the boundary conditions for the computational domains. The inlet and outlet of the house were set for constant velocity and pressure conditions, respectively. The indoor walls were set for no-slip conditions. No buoyancy effects resulting from indoor temperature gaps were taken into account. The analysis was performed under the condition that a constant amount of radon was emitted from the indoor walls. Three-dimensional numerical simulations were carried out using the commercial CFD code STAR-CCM+ Ver. 9. 06. 011. The finite volume method (FVM) was used to discretize the governing equations presented above. The first-order UPWIND scheme was used for the spatial discretization of the governing equations. The SIMPLE algorithm was used to correct the pressure-velocity decoupling.

3. Validation

The validation calculation was performed by comparing the results of the CFD method used in the present study with the results of field measurements taken with a continuous radon monitor by Akbari et al. [10]. In addition, the numerical simulation results of their research and the estimates obtained using the analytical method were compared.

The volume of the house used for the validation calculation was 12×9×2.4 m^3 (Fig. 5). The radon exhalation rate from the surface of the house floor was 65 Bq/m^2/h. Seven vents were installed in the house. Air flowed into the house through the vent in each room.

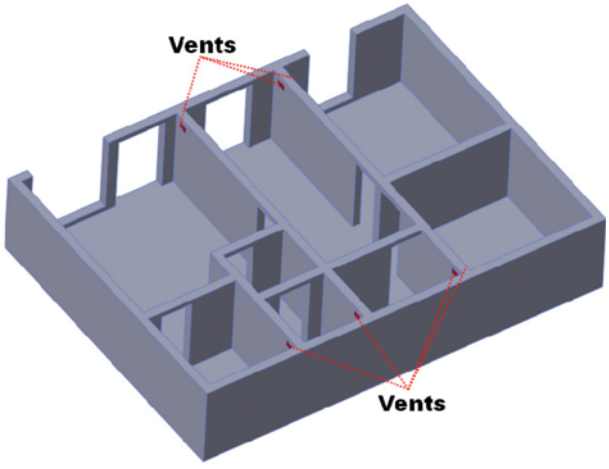

Fig. 5. Computational domain for validation of experiment 1.

The velocity of the air flowing from each vent was obtained using Eq. (16), depending on the size of the room and the ACH, as follows:

$$v = \frac{ACH \times Volume_{room}}{Area_{vent}} \quad (16)$$

Indoor air and radon were able to flow out through the windows and doors. The room doors were assumed to be open.

The steady-state indoor radon concentration was calculated by the following analytical method [19]:

$$C = \frac{EA}{V(\lambda_{Rn} + \lambda_v)} \quad (17)$$

where E is the radon exhalation rate, A is the area of the radon exhalation surface, V is the volume of the house or room, λ_{Rn} is the decay constant of radon, and λ_v is the air change rate in the house.

To validate the numerical procedure, simulations were performed for the house studied by Akbari et al. [10], and the radon concentrations in a room located in the left corner of the house

Table 6. Validation data Unit: Bq/m^3

ACH	Experiment 1				Experiment 2	
	Experimental data	Numerical simulation results of Akbari et al. (% difference*)	Results of the analytical method (% difference*)	CFD results of the present study (% difference*)	Experimental data	CFD results of the present study (% difference*)
0.25	90	107 (18.9)	107.5 (19.4)	98.0 (8.9)		
0.5	45	66 (46.7)	53.8 (19.6)	48.9 (8.7)	86.9	87.7(0.92)
1.2	25	20 (20)	22.4 (10.4)	21.4 (14.4)		

*% difference=(|Experimental data - numerical, CFD or analytical result|)/Experimental data×100

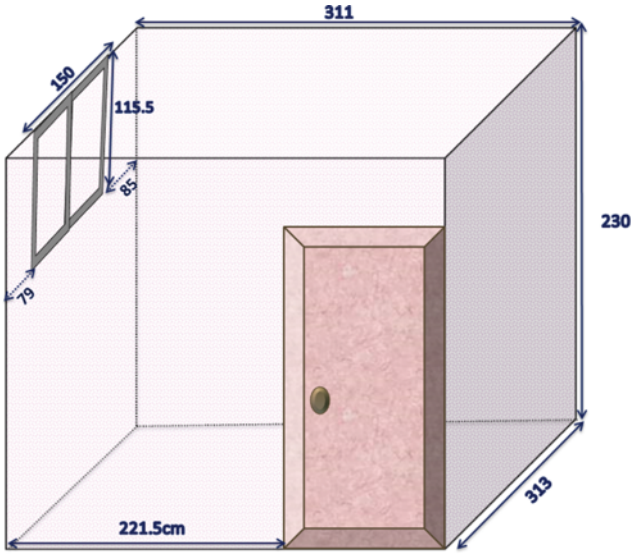

Fig. 6. Computational domain for validation of experiment 2.

were compared. The results of the validation calculation are shown in Table 6. Overall, the present calculation results were much closer to the experimental results than the other results. The maximum difference between the present results and the experimental data was less than 14.4%. Therefore, it seems that the CFD procedures employed in the present study can produce good predictions of the characteristics of the air flow and the consequent indoor radon concentration for the primary calculation.

To validate the present CFD procedure, a radon diffusion experiment was conducted in a closed space. In the experiment, illustrated in Fig. 6, uranium shale was coated on the side walls of a room with dimensions of 3.1×3.1×2.3 m^3. The radon concentration emitted from the sides of the walls was measured using a RAD-7 electronic radon detector. The emission was detected for close to five hours. CFD validation analysis of the indoor radon diffusion was performed under unsteady condition and the calculation conditions were given very similar to the experimental studies. The area of the side wall was 24.9 m^2, and the radon exhalation rate was 112 Bq/m^2-h. As shown in Table 6, the measured indoor radon concentration was 86.9 Bq/m^3, and the indoor radon concentration predicted from the CFD analysis was 87.7 Bq/m^3, with an error margin of 0.92%. Therefore, based on the comparisons with the two sets of experimental data, the computational procedure employed in the present study was judged to be able to predict indoor radon evolution with appropriate accuracy for the purpose of the present study.

RESULTS AND DISCUSSION

1. Regulatory Levels of Indoor Radon

A standard action level for indoor radon is required to evaluate the reduction in indoor radon achieved by ventilation. In South Korea, the recommended level of indoor radon is stipulated in Article 4 of the Enforcement Decree of the Act on the Indoor Air Quality for a public facility as 148 Bq/m^3 [17]. In the U.S, the Environment Protection Agency (EPA) has set a guideline value of 4 pCi/L (148 Bq/m^3) for indoor radon concentrations. This is the action level at which remediation is recommended if the measured value exceeds the guideline value in long-term tests [17]. In addition, the WHO has suggested that the indoor radon concentration be maintained at less than 100 Bq/m^3 [1]. These radon action levels were applied to the evaluation of the indoor quality calculated by the CFD simulation in the present study.

2. Distribution of the Radon Concentration and Ventilation Performance with Respect to the Ventilation System and ACH

In this section, the behavior of the air flow and the distribution of the indoor radon concentration as a function of the ventilation system and ACH were examined. Fig. 7 presents the three-dimensional velocity streamline of the indoor air flow in each case for ACH values of 1.0 and 0.01. A comparison of Figs. 7(a), (c), and (e) shows that the air velocity was lower near the walls in all cases because of the no-slip conditions, and the velocity of the air flow increased after the air passed through the room door, which was a small area. It was possible to observe completely different air streams depending on the ventilation system. Large and slow vortices formed in different parts of the house in each case, and this was a very important factor in the radon concentration. In case 1, a slow rotational flow was formed in the corner in front of the doors of room 1 and the toilet. This rotational flow illustrates the slow convection of the air stream in room 1 and the toilet. In case 2, large and slow vortices also occurred near the toilet and close to the wall on the right side of room 1. In cases 1 and 2, air was supplied through the front or back windows of the house, and this caused the main air flow across the house. In these cases, the configuration of the house geometry resulted in flow separation and a region of flow recirculation against the main flow. In addition, the low-velocity rotational flow produced a zone in which the air flow

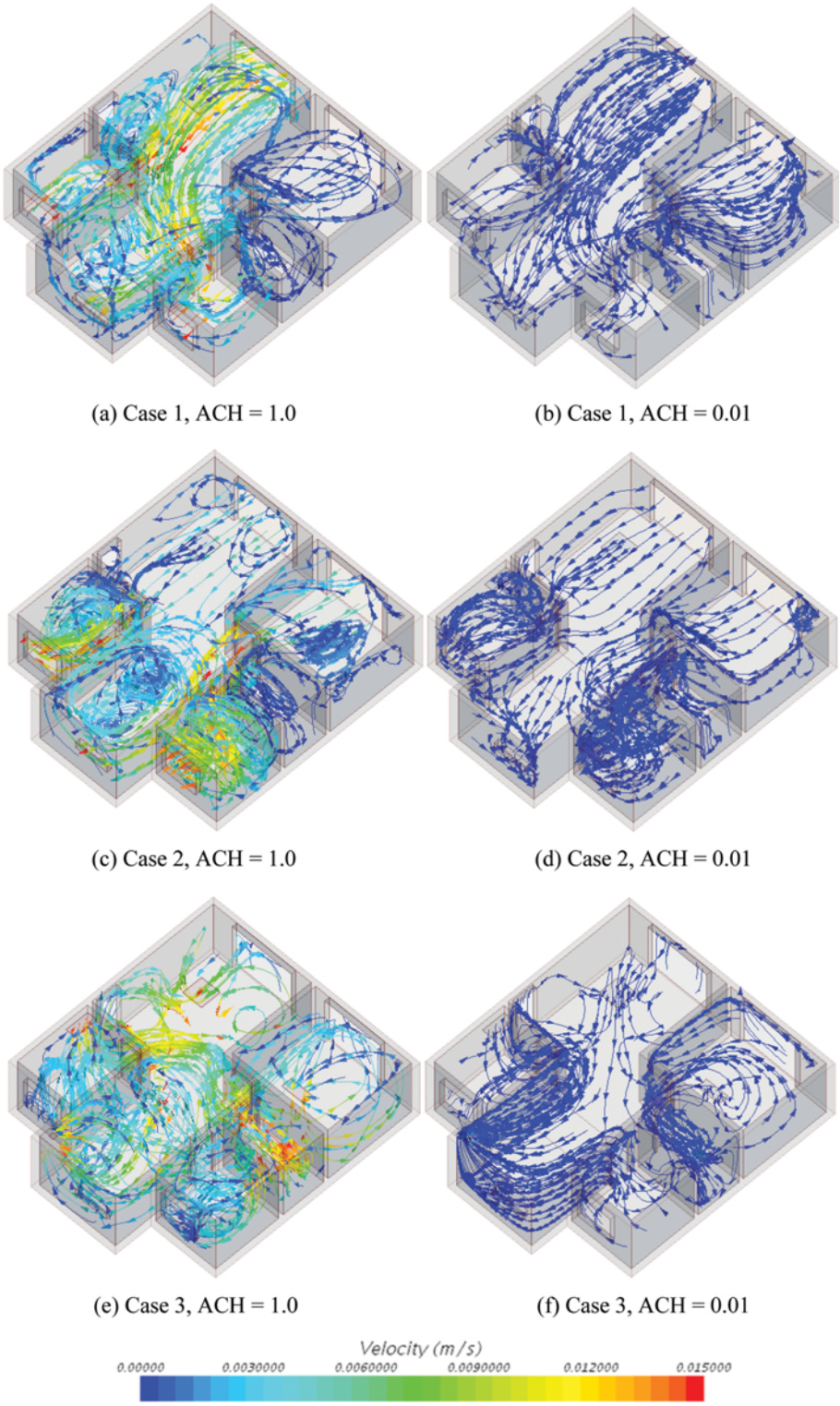

Fig. 7. Velocity streamline of the air flow, depending on the ventilation type and ACH.

was stagnant. The ventilation performance was impeded by these phenomena. On the other hand, it was expected that the ventilation performance would be better with the ventilation conditions of case 3 than with the conditions of the other cases because there was no large, slow vortical region. A comparison of the results with respect to the ACH showed that in all of the cases, the velocity of the air flow in the house decreased as the ventilation rate decreased. Similar flow patterns were observed for ACH values ranging from 0.1 to 1.0. However, in all cases, when the ACH was 0.01, rotational flow barely formed. It is possible that the air velocity was too slow

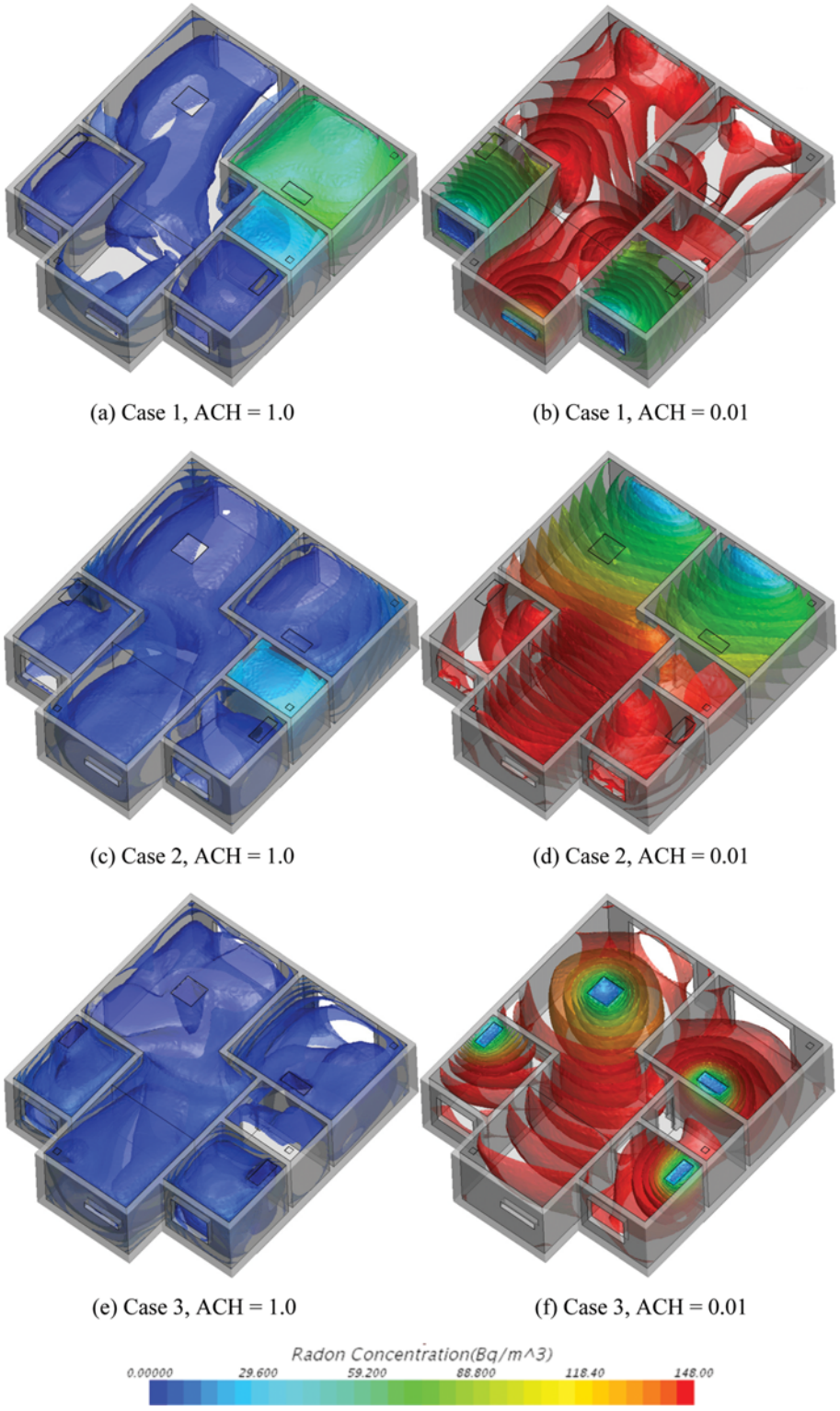

Fig. 8. Contours of the radon concentration, depending on the ventilation types and rates.

to produce flow separation and consequent vortices.

Fig. 8 shows the distribution of the indoor radon concentration as a function of the ventilation rate. For all of the ventilation types, the indoor radon level increased as the ventilation rate decreased from 1 to 0.01 ACH, and clear differences were observed among the ventilation systems. Given the correlation with the air flow, for a rate of 1 ACH, the indoor radon concentration was high where slow flow recirculation occurred. In particular, it was noticeable that radon accumulated more in the toilet and room 1 in case 1 because the indoor air was poorly ventilated, as mentioned before.

In case 2, radon also accumulated in the toilet and close to the wall on the right side of room 1. In addition, the indoor radon concentration decreased in case 3. When the ACH was 0.01, it appeared that the radon concentration could not be further reduced by ventilation. Therefore, an overall high radon concentration was observed in the house, probably because the indoor radon distribution was closely related to the air flow. The radon concentration was lower where the air was supplied or where it entered. On the other hand, the concentration was higher where the air flow velocity was very low or where a dead zone was observed.

A bar chart of the volume-averaged indoor radon concentration for the entire house is presented in Fig. 9. Cases 1-3 are the results of the CFD calculation. In addition, an analytical result was calculated using Eq. (17) and compared with the CFD results. As ACH decreases, the volume-averaged indoor radon level exhibits an increasing trend. The analytical result is similar to the results for cases 2 and 3 for ACH values from 1.0 to 0.1. However, for an ACH of 0.01, the analytical result increased dramatically, from 42 Bq/m^3 to 420 Bq/m^3, and there is a large difference between the CFD results and the analytical value. The difference can be explained as follows. For the CFD simulations, the distribution of the indoor radon concentration was predicted on the basis of not only the ventilation rate but also the various ventilation conditions. In addition, the influence of the internal structure of the house can be included in the CFD simulation, which affects the flow structure. As shown in Figs. 7-8, the flow structure changes depending

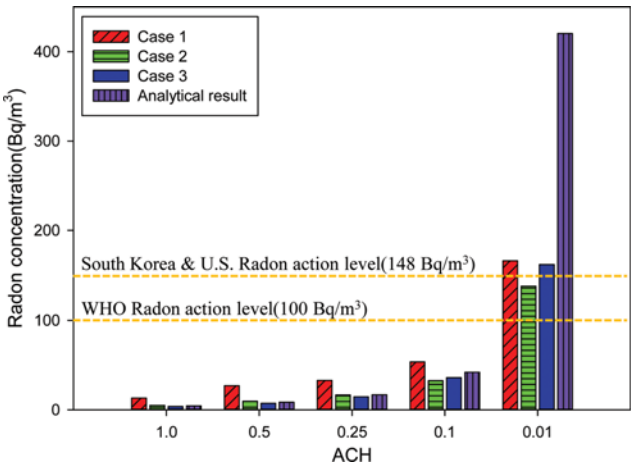

Fig. 9. Volume-averaged indoor radon concentration of the house with respect to ACH.

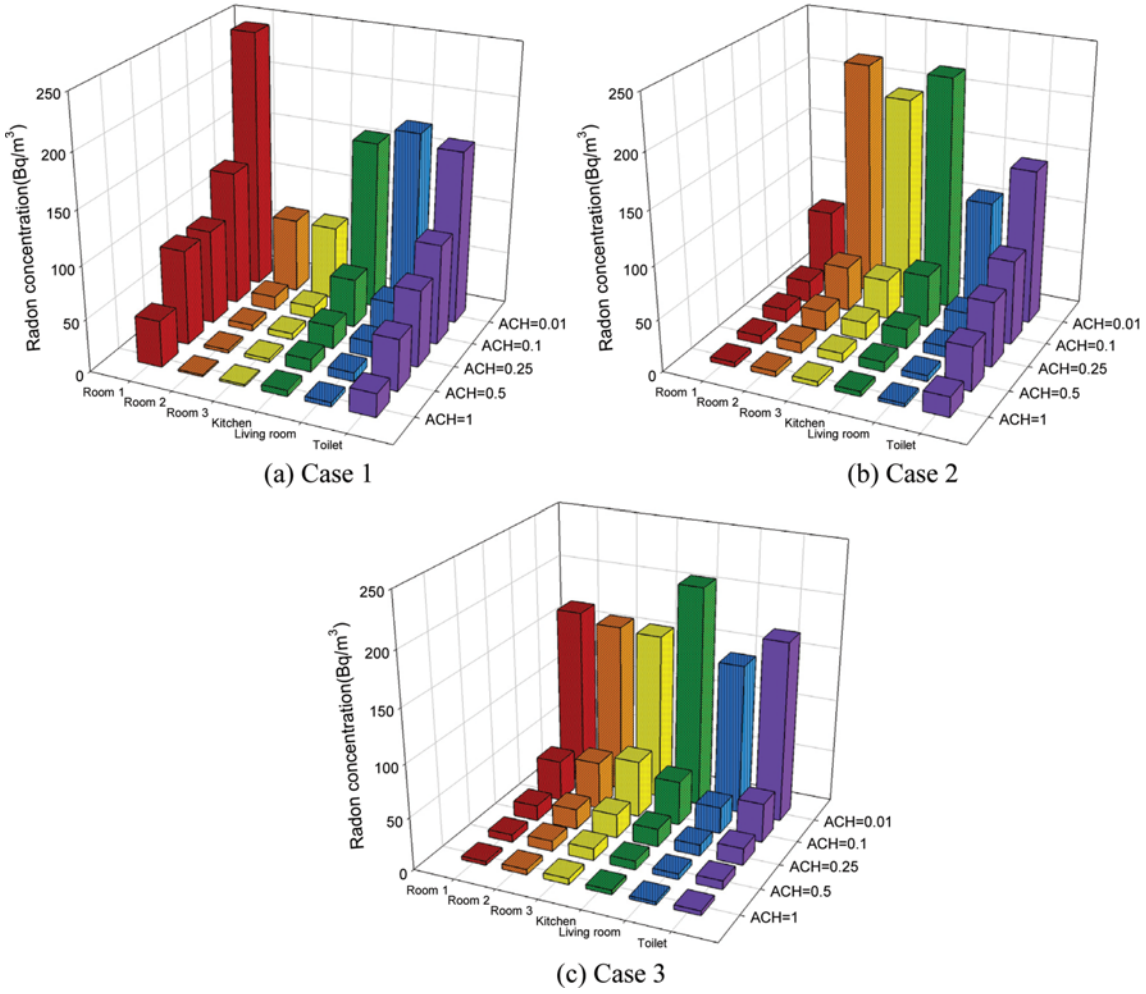

Fig. 10. Volume-averaged indoor radon concentration of each space in the house.

on the ACH, which greatly influences the consequent radon concentration. However, only the ventilation rate was considered in the analytical method. Moreover, the same air change rate was assumed for all rooms. These differences explain the difference between the analytical results and the CFD results. In addition, the radon concentration in each room can be computed and compared by CFD simulation. This is discussed in detail below.

For the purpose of quantitative comparison, the volume-averaged indoor radon concentration in each room is shown in Fig. 10 as a function of the ACH. As mentioned previously, when the ACH was 1.0, regardless of the ventilation type, the concentration of the indoor radon was lower than the action level recommended by WHO. However, in case 1, as the ACH dropped to 0.1, the radon concentration of room 1 exceeded approximately 130 Bq/m^3, and the radon level in the toilet was slightly below the WHO action level. When the ACH decreased to 0.01, the radon concentration dramatically increased, and the radon accumulated to levels above the indoor radon concentration standard in the house, except in rooms 2 and 3. In addition, in cases 2 and 3, as the ventilation rate decreased from 0.1 to 0.01 ACH, the radon concentrations rapidly increased and exceeded the action levels established in South Korea and the U.S. However, the indoor radon concentration could be reduced to a level below the action level at the minimum ventilation rate suggested by the ASHRAE Standard 62.1 or the ventilation regulation of South Korea.

3. Effects of the Inflow Air Angle on the Indoor Radon Concentration

In this section, the effects of the angle of the air inflow through

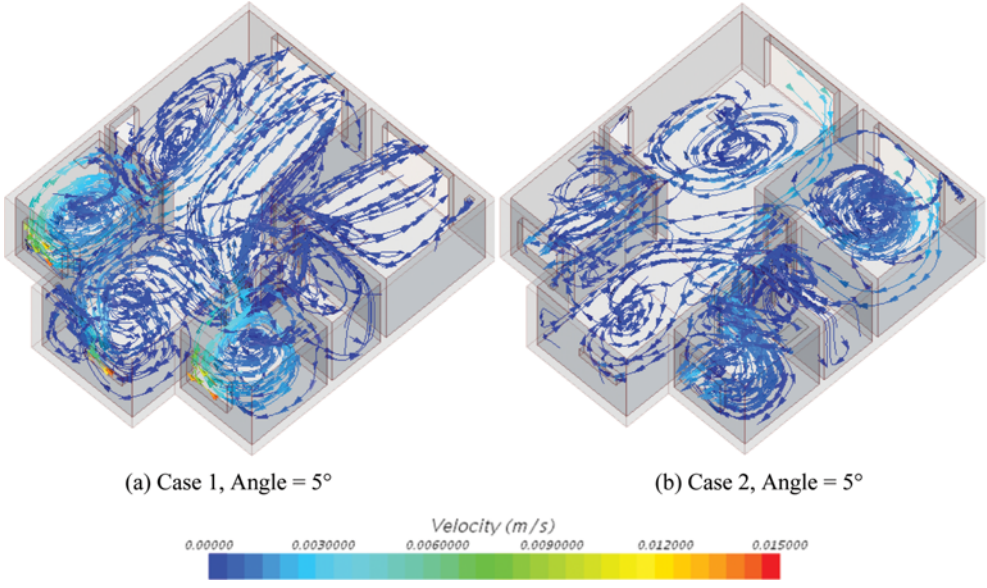

Fig. 11. Stream line of air flow in the house, depending on the angle of inflow air at ACH=1.0.

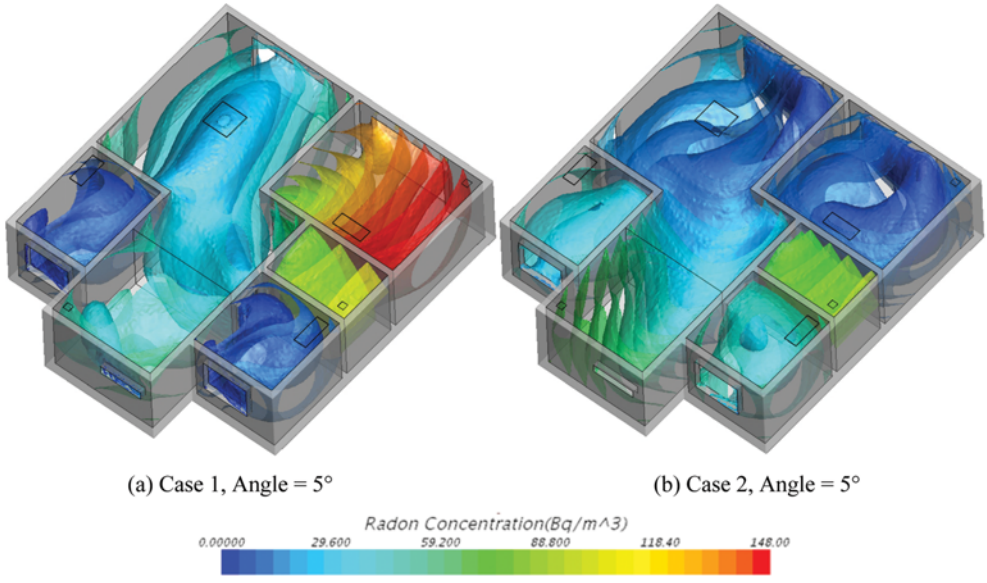

Fig. 12. Stream line of air flow in the house depending on the angles of inflow air into the windows at ACH=1.0.

the windows are discussed. As mentioned before, the influence of the air flow angle was examined under five ACH conditions.

Stream lines of the air flow and the distribution of the indoor radon concentration when the air inflow angle was 5° are shown in Figs. 11 and 12, respectively. A comparison of the results when the angle was 5° (Figs. 7(a) and (b)) with the results for inflow perpendicular to the window (Figs. 7(a) and (c)) shows that in both cases, the air velocity was lower for the inlet angle of 5°. At an inlet angle of 5°, slow rotational flows started to form near the inlets. Finally, the amount of slow rotational flow was larger than in the case of perpendicular inlet flow. As clearly shown, the characteristics of the rotational flow were obviously different, depending on the angle in each case. As Fig. 12 shows, a lower radon concentration was observed in the house when the air velocity was higher. On the other hand, large, slow rotational flow induced a higher radon concentration.

Fig. 13 shows the volume-averaged indoor radon concentration in room 1 and the toilet in case 1 and in the kitchen in case 2, depending on the angle of the air inflow through the windows. In those rooms, distinct changes in the radon concentration were observed, depending on the given ventilation conditions. For an ACH of 1, the radon concentration in room 1 was higher when the angle was as small as 5° or as large as 175°. For both of the angles, the radon concentration exceeded the WHO standard, at approximately 130 Bq/m^3, in room 1. On the other hand, the radon level was maintained at a value lower than the WHO action level in the cases of other angles. When the ACH was 1, the radon level was below the WHO action level in the toilet in case 1 and in the kitchen in case 2, for every angle. However, the indoor radon concentration at an ACH of 0.5 was below the action level of the U.S. and South Korea, although it was higher than the WHO action level. In addition, if the ACH was lower than 0.25, a reduction in the indoor radon sufficient to reach a safe level could not be accomplished in many cases and various angles. The indoor air flow may have been affected by the angle of the air inflow through the windows. This resulted in differences in the indoor radon reduction performance.

The volume-averaged indoor radon concentration of the entire house as a function of the air inflow angle is presented in Fig. 14. The figure illustrates the symmetric distribution of the radon concentration with respect to the angle, with the case of 90° considered to represent the central axis. In both ventilation systems, the radon concentration in the house was below 100 Bq/m^3. In addition, when the ACH was 1.0, the radon concentration did not exhibit a tendency to increase or decrease with a change in the air inflow angle except for angles of 5° and 175°. However, at the lowest, ACH,

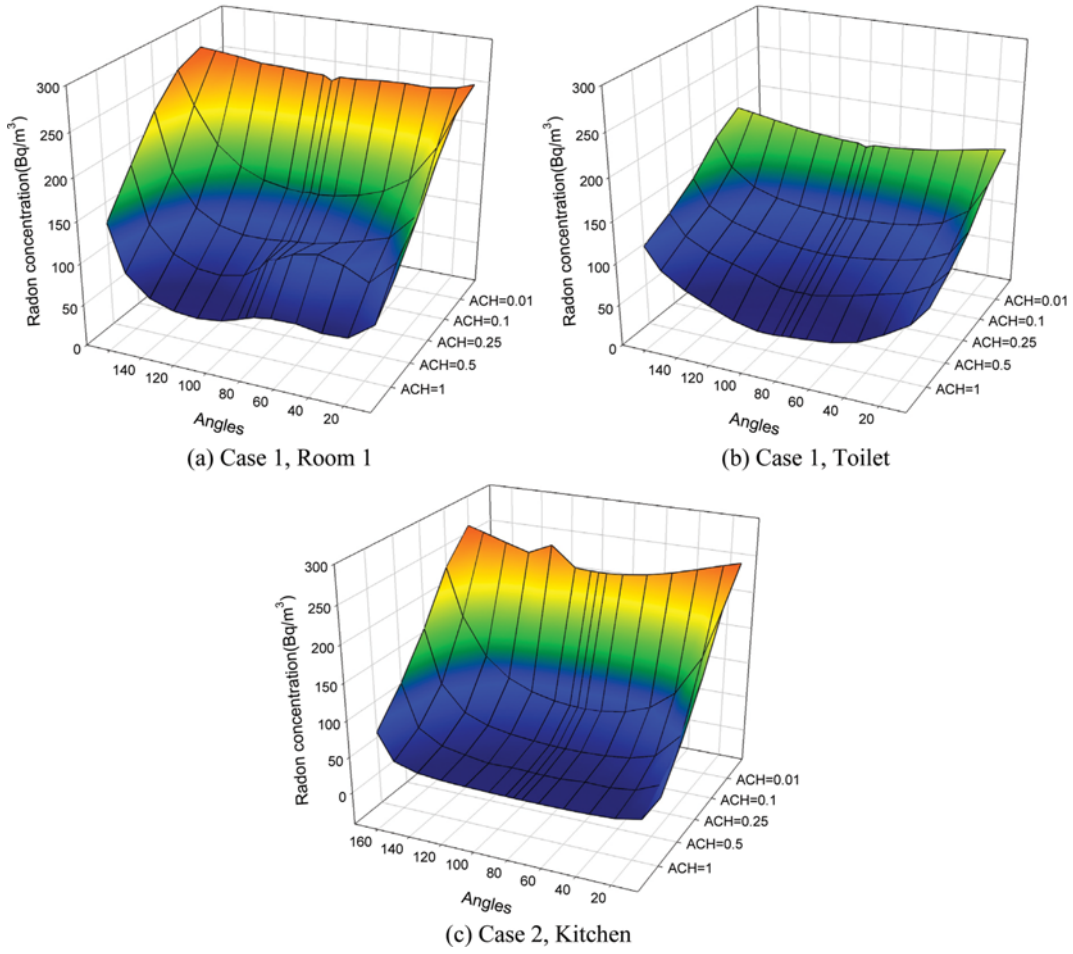

Fig. 13. Volume-averaged radon concentration in a specific area of the house, depending on the angles and ventilation rates.

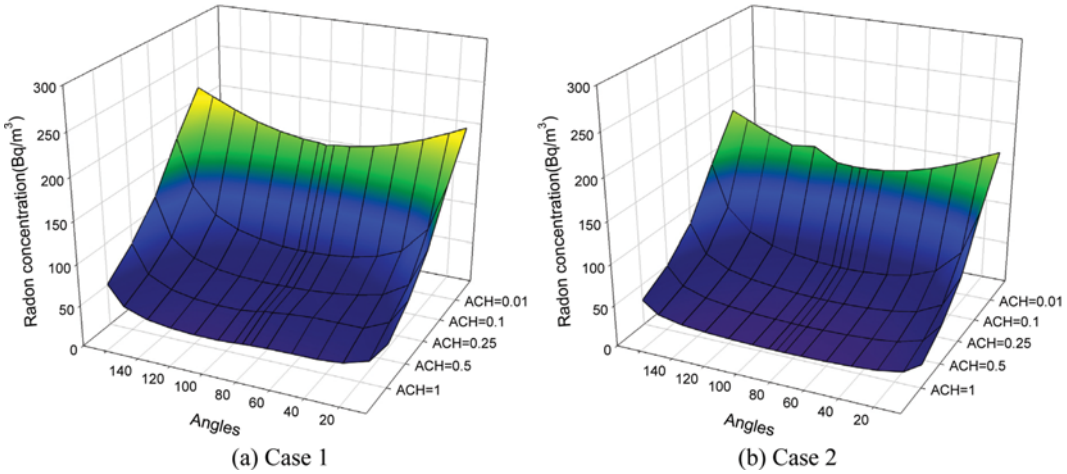

Fig. 14. Volume-averaged indoor radon concentration, depending on the angle of air inflow.

an increasing trend in the radon concentration was clearly observed as the angle became smaller. The total volume-averaged radon concentration was below the regulatory limits, but for each room, cases of concentrations exceeding the limits were possible. These findings are cause for concern for human health.

4. Effects of the Window Opening Area on the Indoor Radon Concentration

We compared the indoor radon concentration for window openings of 25, 50, and 100% under natural ventilation conditions. A CFD analysis was performed for the case1 conditions and ACH=1. The opening area at the front windows of the house was changed while the air volume flow rate was held constant. Fig. 15 presents the volume-averaged radon concentration for window opening percentages of 25%, 50%, and 100%. When the window opening area increased from 25% to 50%, the radon concentration in room 1 increased to 0.4%, which suggests that there were no large changes in the concentration of radon. When the opening area increased to 100%, the radon concentration increased to 24.4% in room 1. The radon concentrations in room 2, room 3, and the living room were not greatly influenced by the open space of the windows.

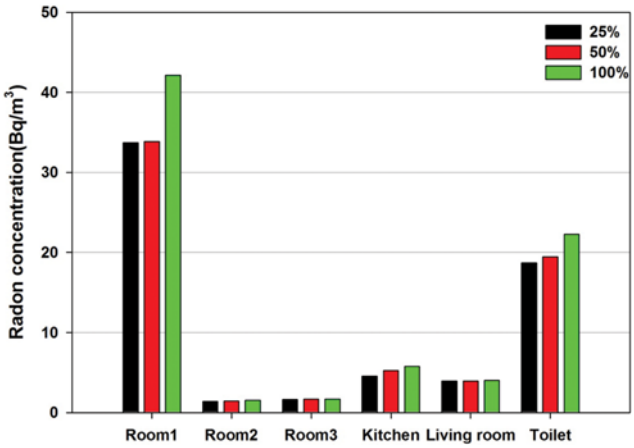

Fig. 15. Volume-averaged indoor radon concentration, depending on the window opening area.

The radon concentrations in the kitchen and toilet increased to 15.9% and 3.9%, respectively, when the window opening area increased from 25% to 50%. When the window was opened 100%, the radon concentration in the kitchen and toilet increased to 9.9% and 14.4%, respectively. The difference in the radon concentration with respect to the window opening is due to the change in the indoor air flow velocity, because the air flow velocity increases as the window opening area decreases.

CONCLUSIONS

Indoor radon concentration distributions and the radon reduction performance of ventilation systems have been scrutinized with respect to ventilation rates and the types and angles of air inflow. Computational fluid dynamics was used to simulate an indoor environment.

At a given ventilation rate, the mechanical ventilation system was more effective in reducing indoor radon than the natural ventilation system. For the same ventilation type, as the ventilation rate increased, the average indoor radon concentration decreased. When the ACH was 1, the indoor radon concentration was maintained below the limit of 100 Bq/m^3 suggested by the WHO by all ventilation types. However, as the ACH decreased to 0.01, the average indoor radon concentrations in some areas exceeded 148 Bq/m^3, which is the regulatory limit in South Korea and the U.S. When air was supplied from the back windows of the house, the effect of the air inflow angle on the distribution of the indoor radon concentration was very slight. However, when air flowed into the house through the front windows, the radon concentration in some parts of the house was high, depending on the air inflow angle. Even for air inflow angles of 5^o and 175^o, the volume-averaged radon concentrations in some areas exceeded the WHO action level. Based on the results, the appropriateness of the minimum ventilation rate according to the standard could be numerically tested. The indoor radon concentration was effectively reduced when the ventilation rate met the U.S. standard or the regulation of South Korea. However, the radon concentration was dramatically changed by varying the ventilation conditions. Furthermore,

a steady-state condition was assumed in the present study, and various factors associated with real ventilation situations were neglected, such as the sizes of the window openings for natural ventilation or the operating time of fans. To achieve more accurate simulation results, it is necessary to calculate the variation in the air flow and the indoor radon concentration distribution over time. In addition, various types of furniture and facilities in a house can affect the air flow. Therefore, further studies that take into consideration conditions and factors such as those mentioned before are needed.

ACKNOWLEDGEMENTS

This work was supported by the Korean Ministry of Environment (MOE) as part of the "Eco Health Action Program".

NOMENCLATURE

C : closure coefficient
D : diffusion coefficient
G_k : turbulent production
J : diffusion flux
k : turbulent kinetic energy
P : pressure [pa]
Re_y : wall-distance-based Reynolds number
S_i : source term
S_{ij} : strain rate tensor
t : time
U : mean velocity vector [m s^{-1}]
u : velocity fluctuation
V : volume [m^3]
v : velocity [m s^{-1}]
Y : mass fraction
σ_k, σ_ε : turbulent schmidt numbers
ε : turbulent dissipation rate
μ : dynamic viscosity
μ_t : turbulent viscosity
ρ : density [kg m^{-3}]
δ : kronecker delta

REFERENCES

1. World Health Organization, *WHO Handbook on Indoor Radon: a Public Health Perspective*, WHO Press, France (2009).
2. S. Page, *J. Environ. Health*, **56**, 27 (1993).
3. International Agency for Research on Cancer, *IARC Monographs on the Evaluation of Carcinogenic Risks to Humans: Man-made Mineral Fibres and Radon*, IARC Press, U.K. (1988).
4. International Agency for Research on Cancer, *IARC Monographs on the Evaluation of Carcinogenic Risks to Humans: Ionizing Radiation, Part 2: Some Internally Deposited Radionuclides*, IARC Press, UK (2001).
5. S. H. Jung, Y. C. Ahn, Y. C. Lee and J. K. Lee, *Korean J. Chem. Eng.*, **30**, 2 (2013).
6. B. Deng, S. Tang, J. T. Kim and C. N. Kim, *Korean J. Chem. Eng.*, **27**, 4 (2010).
7. J. B. Fang and A. K. Persily, *Computer simulations of airflow and radon transport in four large buildings*, National Institute of Standards and Technology (1995).
8. W. Zhuo, T. Iida, J. Moriizumi, T. Aoyagi and I. Takahashi, *Radiat. Prot. Dosim.*, **93**, 357 (2001).
9. F. Wang and I. C. Ward, *Build. Environ.*, **35**, 615 (2000).
10. K. Akbari, J. Mahmoudi and M. Ghanbari, *J. Environ. Radioact.*, **116**, 166 (2013).
11. Statistics Korea, *2013 Social Indicators in Korea* (2014).
12. Ministry of Land, Infrastructure and Transport, *2012 Korea Housing Survey* (2012).
13. Y. J. Ju, *The measurement of radon-222 concentration for release gas into the atmosphere from the building material*, Master Thesis, Chosun University, Department of Nuclear Engineering (2012).
14. C. H. Min, *A Study on the trend of interior finishing materials appeared in apartment model house*, Master Thesis, Yonsei University, Department of Housing and Interior Design (2003).
15. H. R. Yoo, A Survey Study on the Preference of Interior Materials for Multi-Family Housing-Focused on the Medium and Small-sized Apartment in Pangyo newtown in Gyeonggi Province, Master's Thesis, Seoul National University of Science and Technology, Department of Housing Planning and Design (2006).
16. American Society of Heating, Refrigerating and Air-Conditioning Engineers, Inc., ANSI/ASHRAE Standard 62.1-2013 Ventilation for Acceptable Indoor Air Quality (2013).
17. National Legal Information Center, http://www.law.go.kr/main.html.
18. Korea Meteorological Administration, *Annual Climatological Report* (2013).
19. C. K. Man and H. S. Yeung, *Build. Environ.*, **32**, 351 (1997).